5. Articles III.: The shape of the functional response

5.1. Food-web connectance and predator interference dampen the paradox of enrichment

a) Summary

Classic consumer-resource models with hyperbolic functional responses predict that enrichment increases the average biomasses of the species, but eventually leads to species' extinction due to accelerated oscillations (''paradox of enrichment''). However, empirical studies have stressed the complexity of natural food webs and the dominance of sigmoid or predator-interference functional responses, which may dampen population oscillations due to enrichment. Using analytical and numerical methods, we study enrichment effects on simple consumer-resource pairs and complex food webs with hyperbolic Holling type II (hereafter: type II), sigmoid Holling type III (hereafter: type III) and Beddington-De Angelis predator-interference functional responses (hereafter: BDA). Consumer-resource systems with a type III or BDA functional response are highly robust against accelerated oscillations due to enrichment, and the ''paradox of enrichment'' is resolved under certain parameter combinations. Subsequently, we simulated complex food webs with empirically-corroborated body-size structures of consumers that are ten times larger than their average resource. Our analyses demonstrate positive connectance-stability relationships with BDA or type III functional responses. Moreover, increasing connectance of these food webs also increases the robustness against enrichment in models with a BDA functional response. These results suggest that the well-known destabilising effects of connectance and enrichment found in classic models with type II functional responses may be inverted into stabilising effects in more realistic food-web models that are based on empirically-corroborated body-size structures and BDA or type III functional responses.

b) Introduction

The effect of nutrient enrichment (hereafter: enrichment) on natural ecosystems is an important and often discussed subject in both theoretical and applied ecology. Rosenzweig (1971) demonstrated that with increasing enrichment the population dynamics of consumer-resource models are driven from equilibrium dynamics over a bifurcation boundary (hereafter: Hopf boundary) into limit cycle dynamics. With increasing enrichment the amplitudes of the

limit cycles increase, the minima decrease, and populations become more prone to extinction (Rosenzweig 1971; Gilpin 1972). This so called ‘‘paradox of enrichment’’ has received only mixed empirical support (McAllister et al. 1972; McCauley & Murdoch 1990; Bohannan & Lenski 1997; Fussmann et al. 2000; Persson et al. 2001; Trzcinski, Walde, & Taylor 2005). This suggests that enrichment effects on consumer-resource systems in natural communities differ from the predictions of simple model analyses. Opposed by empirical findings (McAllister et al. 1972), Rosenzweig (1972) suggested several effects that might remove the paradox of enrichment in natural communities, which include predator interference and prey-refuges. Another potential explanation for the disparity between theoretical and empirical findings is that the more complex structure of natural food webs might reduce top-down pressure (Polis & Strong 1996; Persson et al. 2001).

Subsequent theoretical studies resolved the ‘‘paradox of enrichment’’ by exploring how population dynamics may be dampened through explicit refuges for the resource populations that are caused by less palatable (Genkai-Kato & Yamamura 1999), inedible (McCauley & Murdoch 1990), invulnerable (Abrams & Walters 1996), inducibly defended (Vos et al. 2004) or spatially separated resource subpopulations (Scheffer & De Boer 1995; Jansen 1995). In homogeneous models of well-mixed populations, implicit refuge effects can be introduced through a type III functional response (Holling 1959b; Scheffer & De Boer 1995). In contrast to models with type II functional responses, these implicit refuge effects remove the paradox of enrichment under a type III functional response - except for the lowest consumption rates (Yodzis & Innes 1992) and increase the persistence of species in models of complex food webs (Williams & Martinez 2004a). Predator-interference functional responses (Beddington 1975; De Angelis et al. 1975) that may be common in natural predator-prey interactions (Skalski & Gilliam 2001) also dampen population cycles and resolve the ‘‘paradox of enrichment’’ under certain parameter combinations (Ruxton, Gurney, & de Roos 1992; Huisman & De Boer 1997; Murdoch et al. 1998; Arditi et al. 2004). Ratio-dependent functional responses also resolve the ‘‘paradox of enrichment’’ (Arditi & Ginzburg 1989; Huisman & De Boer 1997), but lack a mechanistic basis (Abrams 1994).

Moreover, natural consumer-resource systems are embedded in the complex interaction structures of food webs. Theoretical approaches have demonstrated that food-web complexity can greatly modify the stability and strength of consumer-resource interactions (Fussmann & Heber 2002) and may stabilize complex food webs (Haydon 2000). In the same vein, empirical studies suggest that the relationship between enrichment and population persistence depends on the food-web structure that modifies the exploitative top-down pressure of the consumer (Leibold & Wilbur 1992; Persson et al. 2001), and omnivory (Diehl 2003; Trzcinski et al. 2005). Interestingly, experimentally increased complexity in pitcher plant communities removed the paradox of enrichment (Trzcinski et al. 2005).

The present study addresses the effects of enrichment on (1) simple consumer-resource pairs and (2) complex food-web models. In both structural systems, we compared enrichment effects between models with type II, type III, and BDA functional responses. Additionally, we varied the strength of top-down pressure (i.e. consumer maximum consumption rate) and connectance in our food-web analyses. We hypothesised that the paradox of enrichment may be removed by refuge effects (type III functional responses), decreased top-down pressure (decreased maximum consumption rates or predator interference) or increased food web connectance.

c) Methods

We study the dynamical behaviour of populations that are coupled by feeding interactions (hereafter: links) in response to enrichment in (1) simple consumer-resource systems and (2) complex food webs. Consistent with previous studies (Brose et al. 2005b; Brose et al. 2006b), the food-web models are built in a four-step process: (1) the link structure is created by a structural model, (2) the trophic levels of the populations are calculated from the link structure, (3) the body masses of the populations are calculated based on constant consumer-resource body-mass ratios and the trophic levels of the populations, and (4) the parameters of the dynamic consumer-resource model are allometrically parameterised by the body masses of the populations. This framework allows analysing enrichment effects on population persistence in complex food webs.

Complex food-web models

The consumer-resource link structure of the food webs follows three structural models # the cascade model (Cohen et al. 1990), the niche model (Williams & Martinez 2000), and the nested hierarchy model (Cattin et al. 2004). These stochastic models are based on algorithms that arrange trophic links, L, among species based on species richness, S, and connectance, $C=L/S^2$, as input parameters. The food-web structures predicted by the food-web models have been successfully tested against empirical data (Williams & Martinez 2000; Cattin et al. 2004). The feeding matrices created by the food-web models are used to calculate the trophic levels of the species in the food webs as prey-averaged trophic levels (Williams & Martinez 2004b). Generally, the number of producer species varies substantially and systematically with species richness, and connectance. While this has important consequences for species' persistence, the present study aims to analyse enrichment effects independent of the number of producer species. Thus, the confounding effect of a variable number of producer species was removed by selecting the particular subset of the model food webs that contains five producer species.

Consumer-resource model

The population dynamics within these food webs follow a consumer-resource model (Yodzis & Innes 1992) that was updated with new allometric coefficients (Ernest et al. 2003; Brown et al. 2004) and extended to multi-species systems (Brose et al. 2005b; Brose et al. 2006b), where

$$B'_i = r_i G_i B_i - \sum_{j=consumers} x_j y B_j F_{ji} / e_{ji} \quad (5.1.1a)$$

$$B'_i = -x_i B_i + \sum_{j=resources} x_i y B_i F_{ij} - \sum_{j=consumers} x_j y B_j F_{ji} / e_{ji} \quad (5.1.1b)$$

describe changes in relative biomass densities of primary producer (Eqn. 5.1.1a) and consumer species (Eq. 5.1.1b). In these equations, B_i is the biomass density of population i, r_i is i's mass-specific maximum growth rate, G_i is i's logistic growth rate (Eqn. 5.1.6), y is the maximum consumption rate of the consumers relative to their metabolic rate, e_{ji} is j's assimilation efficiency when consuming population i. The functional response, F_{ij}, describes the realised fraction of i's maximum rate of per capita consumption achieved when consuming species j:

$$F_{ij} = \frac{\Omega_{ij} B_j^h}{1 + wB_i + \sum_{k=resources} \Omega_{ik} B_k^h} \quad (5.1.2)$$

where Ω_{ij} is the proportion (0-1) of i's maximum consumption rate targeted to consuming j, h is the Hill exponent which regulates the shape of the curve from Holling type II (h=1) to Holling type III (h=2) functional response (Real 1977), and w quantifies predator interference (Beddington 1975; De Angelis et al. 1975). The predator-interference term in the denominator quantifies the degree to which individuals within population i interfere with one another's consumption activities, which reduces i's per capita consumption if $w > 0$. We used uniform relative consumption rates for consumers with n resources (Ω_{ij} = 1/n) - that is, consumers do not have an active resource preference, but rather feed according to the relative biomasses of their resource species. During dynamical simulations resources may become extinct, which does not change preferences, because consumers still search for all resources (n = const.). This approach excludes adaptive or evolutionary effects on preferences. The per unit biomass biological rates of production, R, metabolism, X, and maximum consumption, Y, follow negative-quarter power-law relationships with the species' body masses:

$$R_p = a_r M_p^{-0.25} \quad (5.1.3a)$$

$$X_{c,p} = a_x M_{c,p}^{-0.25} \quad (5.1.3b)$$

$$Y_c = a_y M_c^{-0.25} \quad (5.1.3c)$$

where a_r, a_x and a_y are allometric constants, M is the average body mass of individuals within the population, and the subscripts c and p indicate consumer and producer parameters, respectively. The time scale of the system is defined by setting the mass-specific growth rate of the basal population to unity. Then, the mass-specific metabolic rates of all species are normalised to this time scale, and the maximum consumption rates are normalised by the metabolic rates:

$$r_i = 1 \tag{5.1.4a}$$

$$x_i = \frac{X_c}{R_p} = \frac{a_x}{a_r}\frac{M_c}{M_p}^{-0.25} \tag{5.1.4b}$$

$$y_i = \frac{Y_c}{X_c} = \frac{a_y}{a_x} \tag{5.1.4c}$$

Inserting Eqn. 5.1.4a-c into Eqn. 5.1.1a-b yields a population dynamic model with allometrically scaled parameters. In food webs with constant consumer-resource body-mass ratios, Z, the body masses M_c of consumers increase ($Z > 1$) or decrease ($Z < 1$) with increasing trophic levels, T by:

$$M_c = Z^{T-1} \tag{5.1.5}$$

The body-masses of the producer species are set to unity and the body-masses of all consumers are expressed relative to the producer masses. Here, we used body-mass ratios, Z, of ten, which characterises consumers that are ten times larger then the mean of size of their resources (note that consumers have a constant average body-mass ratio but varying body-mass ratios to their individual resources). This body-mass ratio is consistent with the geometric mean of 13,101 invertebrate consumer-resource pairs in a global empirical data base (Brose et al. 2005a). The growth of producer species follows a logistic net growth

$$G_i = \left(1 - \frac{B_i}{K_i}\right) \tag{5.1.6}$$

where B_i is the biomass density and K_i is the carrying capacity of the producer species. Knowledge on the trophic levels of the species from the binary feeding matrix predicted by the food-web models (see above under complex food-web models) allows calculating their body-masses relative to the body-mass of the producer species (Eqn. 5.1.5), which parameterises the allometric equations (Eqn. 5.1.4a-c) of the consumer-resource model (Eqn. 5.1.1a-c). We used the following constant model parameters: $e_{ij} = 0.85$ for carnivores and $e_{ij} = 0.45$ for herbivores; $a_x/a_r = 0.314$ for invertebrate consumers in food webs with plants as producer species.

Parameter space

In simple consumer-resource modules (first part) and complex food-web models (second part), enrichment effects were studied by systematically varying the carrying capacity ($-2 \leq \log_{10}(K) \leq 5$). We used continuous relative maximum consumption rates in the consumer-resource modules ($1 \leq y \leq 18$), whereas the complex food webs where studied with three discrete values of y ($y = 1.5$, $y = 10$; $y = 18$). In both parts of the study, we first analysed discrete functional response types - type II ($h = 1$; $w = 0$), type III ($h = 2$; $w = 0$) and BDA ($h = 1$; $w = 1$) - and then studied gradients in predator interference w (0 - 4) and the Hill exponent h (1 - 2). The complex food webs had a fixed number of initial species $S = 30$, thereof the number of producer species was $S_p = 5$. Additionally, we studied the response of complex food webs (discrete functional response types as above and a maximum consumption rate of $y = 10$) to enrichment while varying connectance ($C = 0.075$, $C = 0.15$ and $C = 0.225$). Every simulation started with a random biomass value ($0.05 \leq B_k \leq 1$) for each species, and the number of persistent species ($B_k > 10^{-30}$) was recorded at the end of the time series at t=10,000. Independent simulation runs were carried out with 100 replicates per parameter combination. For every persistent species, we calculated the coefficient of variation (CoVar) within the second half of the time series. For every time series, these values were averaged over the persistent species to yield the mean coefficient of variation.

d) Results

Consumer-resource isoclines

The consumer-resource model (Eqn. 5.1.1a, 5.1.1b) has a resource isocline ($dB_i/dt = 0$) of

$$\ddot{B}_j = \frac{e_{ij}(-\ddot{B}_i + K)(\ddot{B}_i^{\,h+1})}{x_j y K \ddot{B}_i^{\,h-1} + w e_{ij} \ddot{B}_i - w e_{ij} K} \qquad (5.1.7)$$

and a consumer isocline ($dB_j/dt = 0$) of

$$\ddot{B}_i = \left[\frac{w \ddot{B}_j + 1}{y - 1} \right]^{\frac{1}{h}} \qquad (5.1.8)$$

where B_i and B_j are the equilibrium densities of resource and consumer, respectively. In the consumer-resource phase space (Fig. 5.1.1), the fixed point of the model is defined by the intersection of the zero-growth isoclines for positive population densities for resource and consumer ($B_i > 0$; $B_j > 0$). The system is not feasible if the isoclines do not intersect. In systems with prey-dependent functional responses (here: type II and type III), the consumer isocline is independent of resource density (Eqn. 5.1.8, w =0). If these vertical isoclines intersect in declining parts of the prey isocline, the equilibrium is locally stable, whereas intersections in increasing parts of the prey isocline indicate unstable equilibria with oscillatory dynamics (Rosenzweig & Mac Arthur 1963; Rosenzweig 1971). The type II functional response model yields a hump-shaped resource isocline (Fig. 5.1.1A,

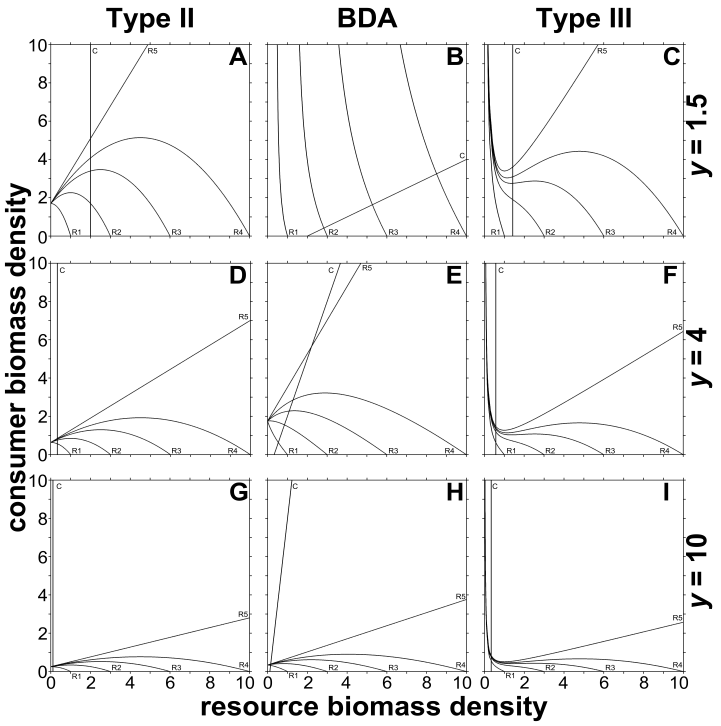

Figure 5.1.1: Isoclines of the consumer-resource model in the phase space of resource biomass density (x-axis) and consumer biomass density (y-axis). Fixed parameters are given in the methods part. Maximum consumption rate y = 1. 5 **(A, B, C)**, y = 10 **(D, E, F)** and y = 18 **(G, H, I)**, type II (**A, D, G** - 1st column), BDA (**B, E, H** - 2nd column) and type III functional responses (**C, F, I** - 3rd column). Each panel shows one consumer isocline (C) and five resource isoclines (R1 - R5) for different carrying capacities (K = 1; 3; 6; 10; 10^{300}).

5.1.1D, 5.1.1G). Enrichment by increasing carrying capacity, K, shifts the resource isocline to higher resource densities, which eventually destabilises the equilibrium point (Fig. 5.1.1A) as shown by Rosenzweig (1971). Increasing maximum consumption rates, y, shift the predator isocline to lower resource biomass densities, which also destabilises the equilibrium (Fig. 5.1.1A, 5.1.1D, 5.1.1G) (Arditi et al. 2004). The type III functional response yields a resource isocline with one or two declining parts: the isocline decreases continuously under low enrichment, whereas it decreases at high resource density to the right of a hump or saddle point and at low resource density to the left of a local minimum or saddle point under high enrichment (Fig. 5.1.1C, 5.1.1F, 5.1.1I). For $y > 2$, the consumer isocline always intersects the resource isocline to the left of the local minimum or saddle point in the decreasing part of the curve, which leads to stable dynamics (Fig. 5.1.1F, 5.1.1I). For $y < 2$ the isoclines can intersect to the right of the local minimum or saddle point in the increasing part of the resource isocline, which yields unstable dynamics for high values of K (Fig. 5.1.1C).

The BDA functional response yields a consumer isocline that increases linearly with resource density (Eqn. 5.1.8, $w = 1$, $h = 1$), and the slope increases with y (Fig. 5.1.1B, 5.1.1E, 5.1.1H). The resource isoclines at high top-down pressure (y) follow a hump-shaped relationship with resource density that is similar to the type II model (Fig. 5.1.1E, 5.1.1H vs. 5.1.1D, 5.1.1G), whereas at low y, the resource isoclines continuously decrease with the resource density (Fig. 5.1.1B). Consistent with the type II model, the system is destabilised by enrichment and top-down pressure. In contrast to the type II model, however, the dynamics are not destabilised by enrichment at low y, because the resource isoclines continuously decline (Fig. 5.1.1B). At higher top-down pressure, the isoclines can intersect in the increasing part of the prey isocline, which does not necessarily indicate instability in systems with a predator-dependent functional response (Arditi et al. 2004). Thus, analytical and numerical analyses are necessary to determine the stability of these systems (see below).

In conclusion, our graphical analyses show that the type II model is generally susceptible to the paradox of enrichment, whereas the type III and BDA models are robust against enrichment for high (y > 2) and low values of the maximum consumption rate, respectively. Interestingly, stable systems with type III functional responses exhibit low population densities (Fig. 5.1.1F, 5.1.1I) with high top-down pressure as shown by Oaten and Murdoch (1975a), whereas stable systems with BDA functional responses have high population densities (Fig. 5.1.1B) at low top-down pressure.

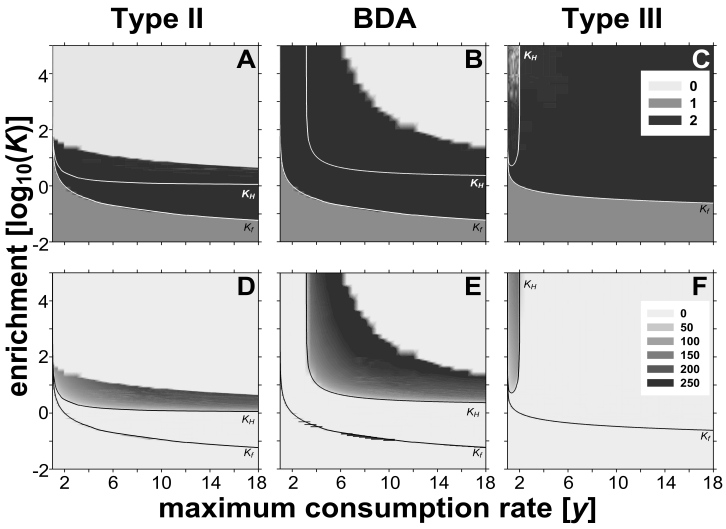

Figure 5.1.2: Numerical and analytical solutions of the consumer-resource model. Panels **A**, **B** and **C** (upper row) show species' survival and panels **D**, **E**, and **F** show their average coefficient of variation (CoVar) depending on enrichment (y-axis) and top down pressure (x-axis) for type II **(A, D)**, BDA **(B, E)**, and type III functional responses **(C, F)**. Analytical boundaries are the feasibility boundary (K_f) and the Hopf boundary (K_H).

Analytical and numerical stability of the consumer resource model.

Subsequently, we extend these equilibrium-based results of the graphical stability analyses by showing (1) analytical solutions of the local stability near equilibrium based on the eigenvalues $\boldsymbol{\lambda}$ of the Jacobian **J** of the system and (2) non equilibrium solutions of numerical simulations of the model. The two-species system is feasible if the biomass densities of both species are positive ($B_i > 0$; $B_j > 0$) and their isoclines intersect. These two conditions are satisfied if the consumer isocline intersects the resource axis (Eqn. 5.1.8: B_i ($B_j = 0$)) between zero and K, which defines a feasibility boundary of

$$K_f = \left(\frac{1}{y-1}\right)^{\frac{1}{h}} \tag{5.1.9}$$

where K_f is the carrying capacity beyond which the system is feasible ($K > K_f$). Interestingly, only the maximum consumption rate, y, and the Hill-exponent, h, affect the feasibility of the system, whereas predator interference, w, has no effect (Arditi et al. 2004).

The Hopf boundary is studied by the Jacobian **J** of the system (Eq. 5.1.1) at its fixed point (B_i, B_j). If the real parts of both eigenvalues $\boldsymbol{\lambda}_{1,2}$ are smaller than zero the system is locally stable, whereas oscillatory behaviour is indicated by a value of the real part of at least one eigenvalue that is larger or equal to zero and a not vanishing imaginary part. The Hopf boundary is given by

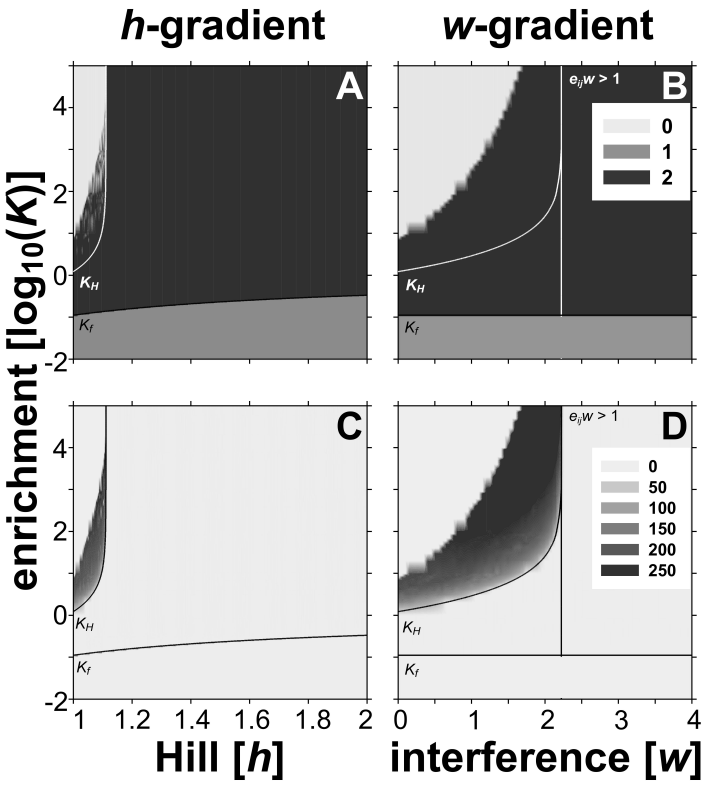

Figure 5.1.3: Numerical and analytical solutions of the consumer-resource model. Panels **A**, **B** (upper row) show species' survival and panels **C** and **D** show their average coefficient of variation (CoVar) depending on enrichment (y-axis) and the Hill-exponent, h, **(A, C)** as well as the predator interference, w, **(B, D)** on the x-axis. Analytical boundaries are the feasibility boundary (K_f), the Hopf boundary (K_H) and the stability boundary for the BDA functional response ($e_{ij}w = 1$).

$$K_H = \frac{(2-h+2(y-1)^{-1})(y-1)^{-\frac{1}{h}}}{1-h+(y-1)^{-1}+x(-1-(y-1)^{-1}+(y-1)^{-1}y)} \quad (5.1.10a)$$

for the Holling functional responses type II and type III and

$$K_H = \frac{x(y-ew+1)^2}{(ew-1)(x(-y+ew-1)(y-1)+yew)} \quad (5.1.10b)$$

A functional response, where K_H is the carrying capacity. Substituting ''1'' or ''2'' for the Hill-exponent, h, in Eqn. 5.1.10a yields the specific Hopf boundaries

$$K_H = \frac{y+1}{y-1} \quad (5.1.10c)$$

$$K_H = \frac{1}{\left(1-\frac{y}{2}\right)\sqrt{y-1}} \quad (5.1.10d)$$

for systems with a type II (Eqn. 5.1.10c) or type III (Eqn. 5.1.10d) functional response. $K_H \rightarrow \infty$ yields $y = 2$ for the type III functional response (Eqn. 5.1.10d) and y $\approx$ 3.17189 for the BDA functional response with a predator interference value of $w = 1$ (Eqn. 5.1.10b).

The stability of the BDA functional response model was analysed using the Routh-Hurwitz criteria: The trace of the Jacobian **J** has to be smaller than zero (Tr **J** = $\boldsymbol{\lambda}_1 + \boldsymbol{\lambda}_1 < 0$) and the determinant of the Jacobian has to be larger than zero (det **J** = $\boldsymbol{\lambda}_1 * \boldsymbol{\lambda}_1 > 0$, see Arditi et al. 2004 for details). Moreover, in systems with BDA functional responses Tr **J** is always smaller than zero if $e_{ij}w = 1$, which results in stability of the system independent of K (see (Arditi et al. 2004) for details). Figure 5.1.2 and 5.1.3 show the analytically derived feasibility and Hopf boundaries and the results of the numerical simulations in the K-y (Fig. 5.1.2) the K-h (Fig. 5.1.3A, 5.1.3C) and the K-w parameter space (Fig. 5.1.3B, 5.1.3D). Additionally, we added the total stability boundary ($e_{ij}w > 1$) for the BDA functional response (Fig. 5.1.3B, 5.1.3D). The numerical analyses of the consumer-resource model show three different states of persistence: (1) the ''resource state'' when only the resource persists (grey), (2) the ''consumer state'' when the persistence of both species is feasible (black), and (3) the ''extinction state'' when both species become extinct (light grey, Fig. 5.1.2A-C, Fig. 5.1.3A-B). The numerical feasibility boundary separates the resource and consumer states, and the extinction boundary divides the consumer state from the extinction state. To analyse the equilibrium and none equilibrium dynamics of the systems we calculated the average coefficient of variation of the consumer and resource species densities in the numerical time series (Fig. 5.1.2D-F, Fig. 5.1.3C-D). Within the consumer state, the numerical Hopf boundary separates equilibrium from limit cycle dynamics (Fig. 5.1.2D-F, Fig. 5.1.3C-D). Generally, the numerical and

analytical solutions for the feasibility and Hopf boundaries were highly consistent (Fig. 5.1.2 and 5.1.3), whereas only the numerical analyses provided extinction boundaries. The exact location of these extinction boundaries is critically dependent on the minimum biomass densities that lead to population extinction (here: $B_{i,j} = 10^{-30}$). Decreasing this extinction threshold would shift the extinction boundary to higher values of K or lower values of y. Generally, our numerical results support the conclusions of the graphical isocline analyses: (1) enrichment increases oscillations with type II functional responses, which eventually leads to the extinction state independent of top-down pressure (y), (2) oscillations and the extinction state are restricted to high top-down pressure (i.e., $y > 3.17189$; $w = 1$) or low interference with BDA functional responses (Fig. 5.1.2B, 5.1.2E; Fig. 5.1.3B, 5.1.3D) and low top-down pressure ($y < 2$) or a low Hill-exponent (e.g. $h < 1.12$, $y = 10$) with sigmoidal type III like functional responses (Fig. 5.1.2C, 5.1.2F, Fig. 5.1.3A, 5.1.3C).

Food-web persistence

Numerical simulations of the complex food-webs show three different states: (1) the ‘‘resource state’’, where only resource species exist (note that in some replicates one or a few herbivores coexist with the resource species), (2) the ‘‘food-web state’’ that is characterised by complex food webs with multiple trophic levels, and (3) the ‘‘extinction state’’, where most species become extinct (note that in a few replicates food web fragments persisted). The resource state with five producer species at low enrichment (Fig. 5.1.4-5.1.6, upper row) and the food-web state occur under all functional responses (Fig. 5.1.4-5.1.6, upper row), whereas the extinction state is restricted to models with a type II functional response (Fig. 5.1.4A, 5.1.5A). In models with a type II functional response, species richness has a hump-shaped relationship with enrichment. The peak of species richness occurs at lower enrichment values with higher values of y (Fig. 5.1.4A), but it does not depend on connectance (Fig. 8.5A). In models with a type III functional response (Fig. 5.1.4C, 5.1.5C) or predator

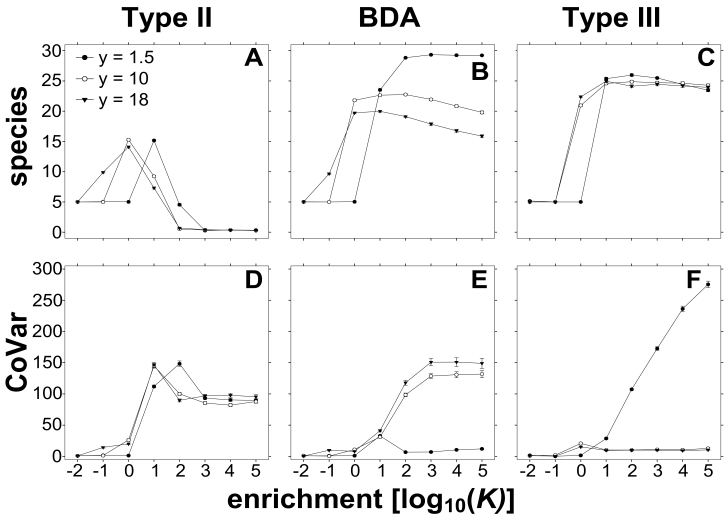

Figure 5.1.4: Complex food-web simulations: species richness **(A, B, C)** and the average coefficient of variation (CoVar) of the persistent species **(D, E, F)** depending on enrichment and the maximum consumption rate, y, (circles: $y = 1.5$; open circles: $y = 10$; triangles: $y = 18$) for type II **(A, D)**, BDA **(B, E)**, and type III functional responses **(C, F)**. Data points show the mean and standard error of 300 replicates.

interference (Fig. 5.1.4B, 5.1.5B) the extinction state does not occur within the range in K simulated here, and species richness is higher than in food webs with a type II functional response. With a BDA functional response, species richness first increases with enrichment in the food-web state, but then declines slightly, except for the lowest maximum consumption rate that leads to almost maximum species richness if the carrying capacity is sufficiently high (Fig. 5.1.4B, y = 1.5, $\log_{10}(K) \geq 3$). In models with a type III functional response, the initial increase is followed by a constant level of species richness for high maximum consumption rates that is robust to further enrichment (Fig. 5.1.4C, y = 10; y = 18), whereas species richness declines slightly with enrichment for a low maximum consumption rate (Fig. 5.1.4C, y = 1.5). In models with a type II functional response, varying connectance (with y = 10) causes only subtle differences in species richness (Fig. 5.1.5A). In models with BDA or type III functional responses, however, increasing connectance (with y = 10) yields higher species richness (Fig. 5.1.5B-C). Additionally, in models with a BDA functional response, the most complex food webs (C = 0.225) show only limited variation in species richness at the saturation level, whereas the least complex food webs (C = 0.075) decrease in species richness under enrichment (Fig. 5.1.5B). In the food-web state, species richness increases with the Hill-exponent until it reaches a saturation level of 25 species (~83% of the initial species richness) at $h \approx 1.4$ (Fig. 5.1.6A). Species richness increases with predator interference up to a saturation level of 30 species (100% of the initial species richness) at w = 4 (Fig. 5.1.6B). Further increases in predator interference (up to w = 10) did not result in differences in species richness. In models with a type II functional response, the coefficient of variation exhibits a hump-shaped relationship with enrichment (Fig. 5.1.4D, 5.1.5D). The fluctuations in the extinction state are caused by food-web fragments in some replicates. In models with a BDA functional response (Fig. 5.1.4E, 5.1.5E), the coefficient of variation increases with enrichment in the food-web state up to a saturation level, except for models with a low maximum consumption rate, in which the coefficient of variation remains at low levels (Fig. 5.1.4E, y = 1.5). In food webs with a type III functional response (Fig. 5.1.4F, 5.1.5F), there was only very limited variation in the coefficient of variation across the enrichment gradient in the food web state, except for models with the lowest maximum consumption rate, in which the coefficient increases with enrichment (Fig. 5.1.4F, y = 1.5). The coefficient of variation decreases with connectance in food webs with predator interference (Fig. 5.1.5E), whereas it does not show a consistent trend under type II or type III functional responses (Fig. 5.1.5D, 5.1.5F). The coefficient of variation decreases in the food-web state with increasing Hill coefficient or predator interference (Fig. 5.1.6C-D).

e) Discussion

There are more than several dozens of different functional response models (Jeschke et al.

2002), and consistent with prior studies (Yodzis & Innes 1992; Arditi et al. 2004; Fussmann & Blasius 2005) our results demonstrate that enrichment effects depend critically on the functional response of the model. Hyperbolic functional response models (e.g. type II model) that differ only slightly exhibit different local stability points, but eventually they are all destabilised by enrichment (Fussmann & Blasius 2005). Consistent with our isocline analyses, this suggests that despite quantitative differences, the qualitative response of hyperbolic functional responses to enrichment is similar. As separate analyses of all possible functional response models would exceed the scope of this study, we have restricted them to some characteristic types: the hyperbolic Holling type II, the sigmoidal Holling type III and the Beddington-De Angelis predator-interference functional response model.

Corroborating prior consumer-resource studies (Rosenzweig 1971; Yodzis & Innes 1992), our results demonstrate destabilising enrichment effects in systems with a type II functional response. Systems with a type III functional response, however, are insensitive to enrichment under intermediate to high top down pressure, because the accelerating per capita consumption of the consumer effectively controls the resource to low equilibrium biomass densities (Oaten & Murdoch 1975a). In contrast, under low top-down pressure the resource escapes the control of a consumer with a type III functional response, which leads to population fluctuations under enrichment (Yodzis & Innes 1992). Under higher top-down pressure ($y > 2$), however, type II functional response models ($h = 1$) are destabilised by enrichment, whereas type III models ($h = 2$) are generally stable. Corroborating Williams and Martinez (2004a), we found that only small increases in the Hill coefficient (e.g. $h \approx 1.12$ for $y = 10$) are necessary to stabilize the population dynamics.

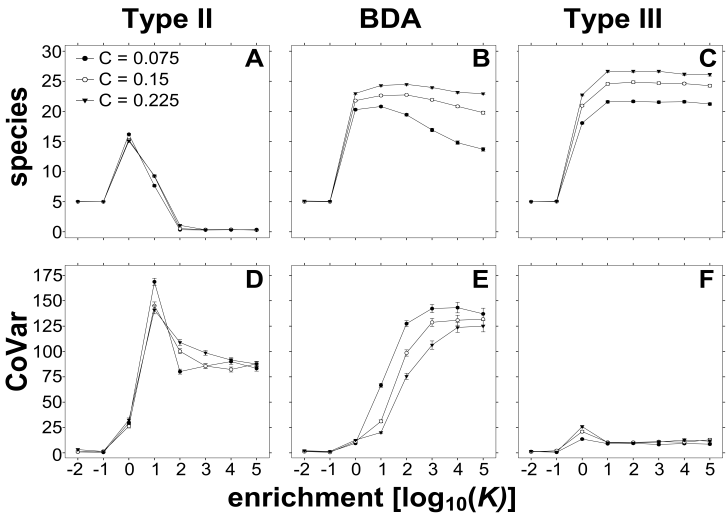

Figure 5.1.5: Complex food-web simulations: species richness **(A, B, C)** and the average coefficient of variation (CoVar) of the persistent species **(D, E, F)** depending on enrichment and connectance C (circles: $C = 0.075$; open circles: $C = 0.15$; triangles: $C = 0.225$). for type II **(A, D)**, BDA **(B, E)**, and type III functional responses **(C, F)**. Data points show the mean and standard error of 300 replicates.

Interestingly, ratio-dependent functional responses that can be deduced from predator-interference models under specific parameters (Skalski & Gilliam 2001; Arditi et al. 2004) also prevent the ‘‘paradox of enrichment’’ (Arditi & Ginzburg 1989; Huisman & De Boer

1997). Due to mechanistic criticism of the ratio-dependent model (Abrams 1994) and better empirical support for the predator-interference model (Schenk et al. 2005), we have focused on the Beddington-De Angelis predator-interference model. Our results corroborate prior studies (Rosenzweig 1972; Ruxton et al. 1992; Huisman & De Boer 1997; Murdoch et al. 1998; Arditi et al. 2004) by showing that predator interference dampens population cycles without entirely preventing the ‘‘paradox of enrichment’’ under high top-down pressure or low interference. Moreover, consumer biomass decreases with increasing predator interference (Arditi et al. 2004), what may lead to consumer extinction at high predator interference values. However, we carried out additional simulations showing that population persistence was not affected up to high predator interference (w = 10; data not shown). Population stability and persistence are critically dependent on the combination of top-down pressure and predator interference in the functional response. Empirically documented values range from zero to 1.6 for predator interference (Skalski & Gilliam 2001) and from 1.6 to 19 for maximum consumption rates (Yodzis & Innes 1992). Within these parameter ranges, our results suggest that predator interference dampens enrichment-driven dynamics thus leading to a higher robustness against enrichment than a type II functional response without causing consumer extinction due to low biomass densities. This effect can be explained by a decreased feeding rate of the consumer due to interference at high consumer densities (Hassell & May 1973; De Angelis et al. 1975).

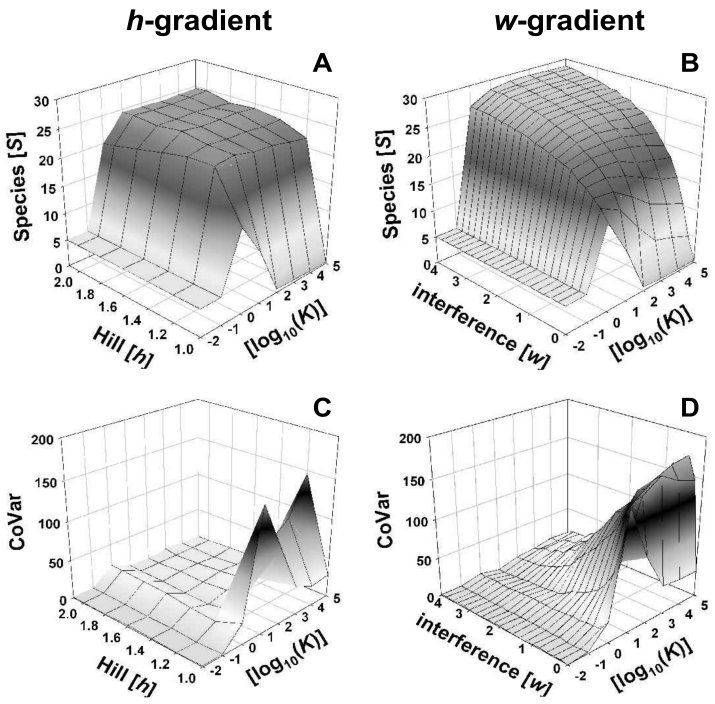

Figure 5.1.6: Complex food-web simulations: species richness **(A, B)** and the average coefficient of variation (CoVar) of the persistent species **(C, D)** depending on enrichment and the Hill-exponent, h, **(A, C)** and predator interference, w, **(B, D)**.

Our simulations of complex food webs and simple consumer-resource modules yielded very consistent results. The mechanistic understanding gained by analysing the simple modules could thus be used to explain the patterns found in the complex food web simulations. Generally, food webs with type II functional responses are highly susceptible to the paradox of enrichment, whereas food webs with type III or BDA functional response are robust against enrichment. Consistent with the modules, food webs with a BDA functional

response and low maximum consumption rates are almost entirely persistent, and food webs with a type III functional response and a low maximum consumption rate (y = 1.5) exhibit unstable dynamics under enrichment.

Interestingly, we found that species richness increases with connectance in food webs with type III or BDA functional responses. This contrasts classic stability analyses with random networks (Gardner & Ashby 1970; May 1972), but corroborates findings that food web connectance may stabilize simple 10-species food webs (De Angelis 1975; Nunney 1980), larger food webs (Haydon 2000) and prevents secondary extinctions (Eklöf & Ebenman 2006). We have used an empirically corroborated body-size structure of consumers that are ten times larger than their average resource (Brose et al. 2006a) for our model communities. Prior analyses have demonstrated that such a body-size structure yields highly stable food webs and positive diversity-stability relationships (Brose et al. 2006b). Our present results suggest that this body-size structure also causes positive connectance-stability relationships.

Moreover, we have simulated food-web structures according to several models: the cascade model (Cohen et al. 1990), the niche model (Williams & Martinez 2000), and the nested-hierarchy model (Cattin et al. 2004). Interestingly, our simulations suggest that there are only marginal and inconsistent differences in species richness between the different food web models (data not shown). In contrast to other studies demonstrating the higher stability of niche-model food webs when compared to the cascade model (Martinez 2006), we have restricted our analyses to those food webs that include exactly five basal species. This condition was necessary to ensure the same enrichment level of replicate runs of the same carrying capacity, because the total enrichment in complex food webs equals the number of basal species times their carrying capacity. As the niche model builds food webs with systematically more basal species than the cascade model, we anticipate that this difference may be responsible for the disparities between our results and prior studies (Martinez 2006).

Corroborating our initial hypothesis, our results demonstrate that more complex food webs with predator interference are more robust against the paradox of enrichment than food webs of lower connectance - except of highly unstable food webs with type II functional responses. Williams and Martinez (2004a) and Brose et al. (2006b) demonstrated that type III functional responses yield population stability and persistence in model food webs at a carrying capacity of one. We have extended these findings across gradients of enrichment and maximum consumption rates. In contrast to Williams and Martinez (2004a), we did not find equilibrium dynamics and persistence of all populations in our simulations of complex food webs with type III functional responses. Potential explanations for this disparity include the higher number of species (30 vs. 10) and the higher consumer-resource body-mass ratios (10 vs. 1) used in our simulations. Interestingly, counter to our findings in simple consumer-resource systems the complex food web models do not exhibit an extinction state under predator

interference (w = 1) at maximum consumption rates of 10 and 18. Again, this remarkable robustness of the complex food webs against enrichment can be mechanistically explained by our findings for simple modules. In our simulations, increasing connectance increases the generality of the consumers (i.e. on average consumers have more prey), which leads to a decrease in their relative preferences for specific prey. The maximum consumption rate and the relative preference are part of the nominator of the functional response (Eqn. 5.1.2). Thus, decreases in both parameters decrease the nominator of the functional response while the denominator (e.g. the half saturation density) remains constant, which decreases the top-down pressure through specific links. Consistent with our consumer-resource simulations, this decrease in top-down pressure for specific links with increasing connectance removes the paradox of enrichment under a BDA functional response. This result is based on the assumption that consumers distribute their relative preferences equally amongst their resources by having the same ability to consume the resource species on the same biomass densities. Deviations from this assumption in natural food webs (Williams & Martinez 2004b) are likely to result in destabilising enrichment effects on a few strong links, whereas the majority of weak links may be unaffected. Exploring link-specific deviations from our assumptions would be important tests of the generality of our quantitative results. However, consistent with our findings under the simplifying assumption of equal relative resource preferences, a recent empirical study has demonstrated that experimentally increased connectance in pitcher plant communities removes the paradox of enrichment (Trzcinski et al. 2005).

Overall, our results suggest that the well-known destabilising effects of connectance and enrichment found in classic food-web studies (Rosenzweig 1971; May 1972) with linear or type II functional responses may be inverted into stabilising effects in food webs with an empirically corroborated body-size structure and predator-interference or type III functional responses. This conclusion gains particular importance as a meta-study demonstrated that predator interference is common in natural consumer resource interactions (Skalski & Gilliam 2001). Furthermore, predator-switching behaviour between multiple resource species in dependence on their abundance converts a type II functional response of a simple one consumer-one resource system into a type III functional response (Murdoch 1969; Real 1977; Elliott 2004). Together, these findings suggest that many consumer-resource interactions in natural food webs might be best characterised by type III and predator-interference functional responses.

Our results corroborate the prior finding that specifying the functional responses of consumer-resource systems (Yodzis & Innes 1992; Fussmann & Blasius 2005) and the connectance of the food web (Polis & Strong 1996; Persson et al. 2001) are of critical importance for predicting the consequences of enrichment in natural ecosystems. Our results

suggest that the paradox of enrichment describes the response of simple food webs or consumer-resource systems in microcosms that characteristically exhibit type II functional responses (Bohannan & Lenski 1997; Fussmann et al. 2000; Persson et al. 2001). In contrast, most natural communities may exhibit a higher connectance, predator-interference or type III functional responses due to prey refuge effects (e.g. habitat connectance or inducible defences), which makes them less sensitive to enrichment (McAllister et al. 1972; McCauley & Murdoch 1990; Leibold & Wilbur 1992; Trzcinski et al. 2005) than predicted by the paradox of enrichment (Rosenzweig 1971).